Theor Chem Acc (2014) 133:1418
DOI 10.1007/s00214-013-1418-9

REGULAR ARTICLE

Density functional study on structures, stabilities, and electronic properties of size-selected Pd_nSi^q ($n = 1$–7 and $q = 0, +1, -1$) clusters

Pakiza Begum · Debajyoti Bhattacharjee · Bhupesh Kr. Mishra · Ramesh C. Deka

Received: 10 May 2013 / Accepted: 29 October 2013

Abstract The density functional theory (DFT) calculations within the framework of generalized gradient approximation have been employed to systematically investigate the geometrical structures, stabilities, and electronic properties of Pd_nSi^q ($n = 1$–7 and $q = 0, +1, -1$) clusters and compared them with the pure Pd_{n+1}^q ($n = 1$–7 and $q = 0, +1, -1$) clusters for illustrating the effect of doping Si atom into palladium nanoclusters. The most stable configurations adopt a three-dimensional structure for both pure and Si-doped palladium clusters at $n = 3$–7. As a result of doping, the Pd_nSi clusters adopt different geometries as compared to that of Pd_{n+1}. A careful analysis of the binding energies per atom, fragmentation energies, second-order difference of energies, and HOMO–LUMO energy gaps as a function of cluster size shows that the clusters Pd_4^+, Pd_4, Pd_8^-, $Pd_5Si^{0,+,-}$, and $Pd_7Si^{0,+,-}$ possess relatively higher stability. There is enhancement in the stabilities of palladium frameworks due to doping with an impurity atom. In addition, the charge transfer has been analyzed to understand the effect of doped atom and compared further.

Keywords Palladium–silicon bimetal · Cluster · Density functional theory · Geometric configuration · Electronic property · Relative stability · HOMO–LUMO gap

1 Introduction

Clusters are aggregates of atoms or molecules which may contain any number of component particles from three to ten or hundreds of millions. A transition metal cluster is particularly important among others because it is expected to show specific magnetic properties and catalytic activity [1]. Mono- or bimetallic nanoclusters have received much interest in scientific research and industrial applications such as catalysis, owing to their unique large surface to volume ratio and quantum size effects [2, 3]. In recent years, late transition metals such as Pd, Pt, and Rh find wide applications in different fields of chemistry particularly in catalysis [4–6].

Palladium, a group 10 element of the periodic table, is nowadays widely used in catalytic converter. In finely divided state, it can enhance the rate of hydrogenation, dehydrogenation reactions, as well as the cracking of petroleum [7]. When dispersed on conductive materials, it is an excellent electrocatalyst for oxidation of primary alcohols in alkaline media [8]. Due to the importance of Pd, various studies have been carried out on Pd clusters as well as other metal atom-doped Pd clusters. Kalita and Deka carried out density functional theory (DFT) study on neutral as well as charged Pd_n ($n = 1$–7) clusters to investigate the stability of these clusters on the basis of structural and electronic properties [9]. They found Pd_4 as the electronically most stable cluster or a magic-number cluster among the clusters studied. Among the studies on metal doping on

Electronic supplementary material The online version of this article (doi:10.1007/s00214-013-1418-9) contains supplementary material, which is available to authorized users.

P. Begum · D. Bhattacharjee · B. Kr. Mishra · R. C. Deka (✉)
Department of Chemical Sciences, Tezpur University, Napaam, Sonitpur, Tezpur 784028, Assam, India
e-mail: ramesh@tezu.ernet.in

P. Begum
e-mail: pakiza@tezu.ernet.in

D. Bhattacharjee
e-mail: debaj@tezu.ernet.in

B. Kr. Mishra
e-mail: bhupesh@tezu.ernet.in

Published online: 19 November 2013

Pd clusters, Barman et al. [10] reported the enhanced magnetic moment as well as binding energy of Pd_n clusters ($n = 1$–13) which results due to doping of iron (Fe). They also found that in the mid-size region ($n = 5$–7), Fe substitution in Pd_n clusters results in a threefold enhancement in the magnetic moment. Wei et al. [11] investigated the effects of doped lead (Pb) atoms on Pd_n clusters ($13 \leq n \leq 116$). The average Pd–Pd bond length of Pd clusters is expanded by $\sim$0.1 Å on doping with Pb. Also the chemical activity of Pb–Pd clusters is greater than the pure Pd clusters as a result of transfer of surface charge population by Pb atoms. The geometric and electronic properties of small Ag_mPd_n clusters with $m + n = 2$–5 are studied within the framework of density functional theory by Kilimis et al. [12]. Their results indicated that for bimetallic tetramers and pentamers, the clusters shift from two-dimensional to three-dimensional structures with the addition of a second Pd atom. From the calculation of the excess energy and second energy difference of bimetallic clusters, Ag_2Pd_2 was identified as the most stable tetramer. These metal-doped bimetallic Pd clusters found wide applications in the field of catalysis [13–15]. Peng et al. [16] have done DFT calculations to investigate CO and O_2 adsorption and CO oxidation on the Au_mPd_n ($m + n = 2$–6) bimetallic clusters. It is found that the adsorption energies of both CO and O_2 on Au_mPd_n ($m + n = 2$–6) are greater than those on the pure gold clusters of corresponding sizes, and unexpectedly greater than those on Pd clusters in some cases. Similarly, the calculated reaction barrier of CO oxidation on Au_2Pd is found to be lower than those on Au_3 and Pd_3, which indicates that Au/Pd bimetallic clusters potentially have a better catalytic activity for CO oxidation.

Till now, only a few studies on non-transition metal-doped Pd clusters are carried out. Among the non-transition metals, silicon is an interesting candidate for doping metal clusters. It is an important element in the field of semiconductor and nanoelectronics. A number of studies on Si-doped transition clusters particularly Au clusters have already being performed [17–21]. But till now no attention was given to study how silicon atom will interact on metallic environment of palladium. As both Si and Pd have individual importance in different fields of science, doping of Si on Pd may give rise to a new scenario among scientific community particularly in the field of catalysis, electronics, etc. Therefore, in this paper for the first time we systematically studied the effect of Si on Pd_n ($n = 1$–7) clusters using DFT. In Sect. 2, we briefly discussed the computational method used. The discussions on the $SiPd_n$ ($n = 1$–7) structures and the electronic properties as well as stability were presented in Sect. 3. The last section is the conclusions. We hope this study would not only be useful for deeply understanding the influence of Si on different properties of Pd but can also provide powerful guidelines for future experimental studies.

2 Theoretical methods and computational details

All DFT calculations were performed using DMol^3 program package [22, 23]. Geometry optimizations and frequency analysis were done by treating the exchange–correlation interaction with generalized gradient approximation (GGA) using Becke–Lee–Yang–Parr (BLYP) [24–26] exchange–correlation functionals. We have used the double numerical with polarization (DNP) [22, 23] basis set for our calculations. The DNP basis set is comparable to Gaussian 6-31G**, but DNP is more accurate than a Gaussian basis set of the same size [27, 28]. Because Pd is a heavy atom, a full electron calculation is rather time consuming. Therefore, the clusters have been investigated using relativistic all electron density functional theory (VPSR) [29] based DNP basis set, which is adopted to describe the $4d^2$ $4p^6$ $4d^{10}$ outermost valence electrons. To improve computational performance, a global orbital cutoff of 4.5 Å was employed. Self-consistent field (SCF) procedures are done with tolerances of the energy, gradient, and displacement convergences: 1×10^{-5} Ha, 2×10^{-3} Ha Å^{-1}, and 5×10^{-3} Å, respectively.

In the view of obtaining the lowest ground-state structures of Pd_nSi clusters, the previous studies on charged and neutral Pd_{n+1} clusters are first employed as guide [9, 30]. We had also taken into consideration the energetically most favorable geometries of the transition metal-doped clusters earlier published in literatures [9, 27, 28, 31]. Ample number of possible initial configurations for each cluster have been considered in geometry optimizations and are relaxed fully without any symmetry constraints. We then considered numerous isomeric structures by substituting one Pd atom in Pd_{n+1} cluster with one M atom, on each possible site, taking into account the previous studies on gold, silicon, and aluminum clusters substituted by various atoms [32–36]. Generally, the clusters with fewer surface atoms and higher symmetry are accepted to be more stable [33]. Considering the spin polarization, every initial structure is optimized at various possible spin multiplicities. For a given initial structure, spin-unrestricted calculations are performed for different spin multiplicities. All geometries have been fully relaxed and vibrational analysis has been carried out intending to resolve the structures to correspond to the local minima in the potential energy surface. The vibrational frequencies are found to be positive for all the structures confirming them to be at energy minima. The zero-point vibrational energy corrections have been included in all the calculations. In this way, a large number of configurations have been optimized, but we

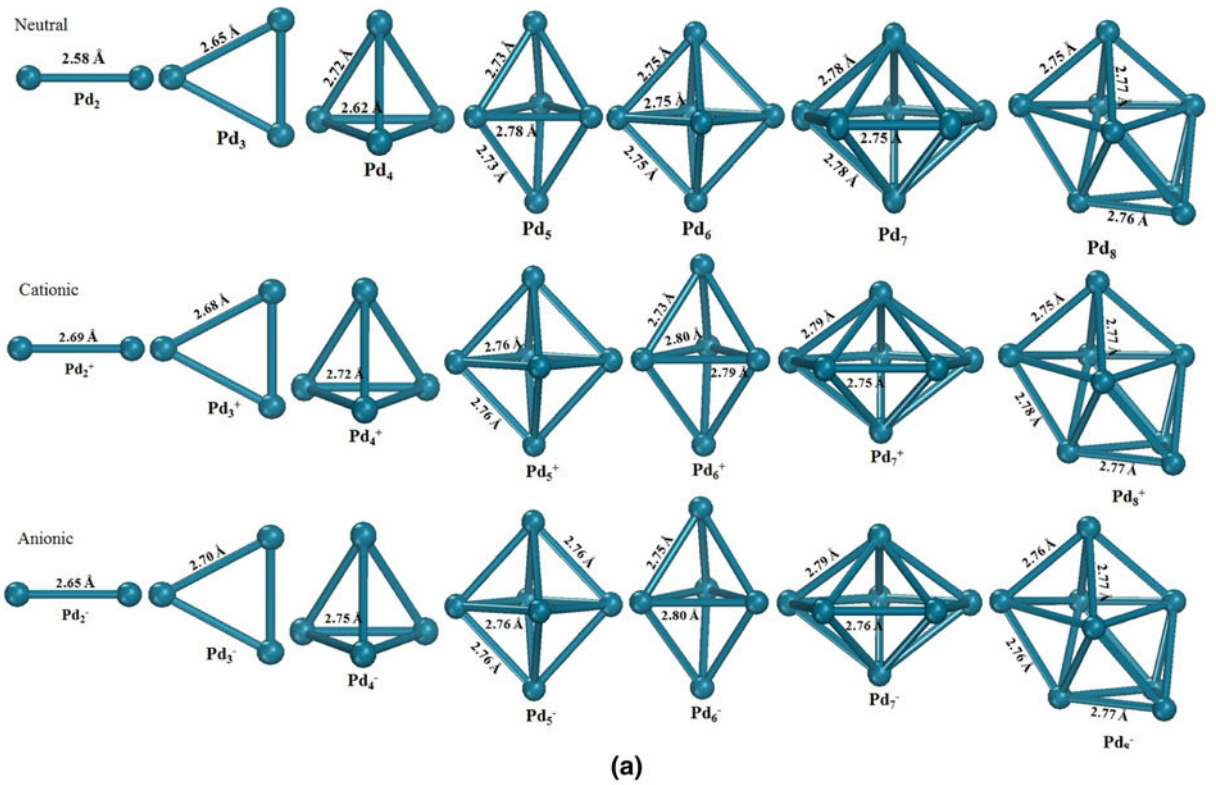

Fig. 1 **a** The optimized structures for the most stable structures of Pd^{q}_{n+1} ($n = 1$–7 and $q = 0, +1, -1$) clusters. **b** The optimized structures for the most stable structures of Pd_nSi^q ($n = 1$–7 and $q = 0, +1, -1$) clusters. The *blue* and *yellow balls* represent Pd and Si atoms, respectively

focus our attention only on the energetically low-lying, i.e., the most stable ones.

We first perform calculations on Pd_{n+1} ($n = 1$–7) clusters in order to discuss the effects of doped impurity atom on palladium clusters. Full geometry optimizations have been done for the neutral clusters at three different spin multiplicities ($M = 1$, 3 and 5) without imposing any symmetry constraints. The lowest energy neutral clusters are then taken to carry out geometry optimizations for singly charged clusters (cationic and anionic) at spin multiplicities $M = 2$, 4, and 6.

In order to obtain the lowest energy doped isomers, initial structures were constructed by substituting a Si atom for one Pd atom in the pure structures at various attaching sites. As mentioned above, for each doped structure also, we have carried out similar calculations for three electronic states with different multiplicities. For the neutral Pd_nSi clusters, we considered the singlet, triplet, and pentet states, whereas for the ionic Pd_nSi^+/Pd_nSi^- clusters, we considered the doublet, quartet, and sextet states. Only the lowest energy structures are discussed in this paper.

3 Results and discussion

The lowest energy structures of Pd_{n+1}^q and Pd_nSi^q ($n = 1$–7 and $q = 0$, $+1$, -1) clusters are presented in Fig. 1. Meanwhile, the detailed information regarding their structural characteristics—the symmetry, spin multiplicity, binding energy, highest occupied–lowest unoccupied molecular orbital (HOMO–LUMO) energy gap, the charge on Si atom, fragmentation energy, and second-order difference of energy—and the population analysis is conducted using the computational scheme described in Sect. 2.

3.1 Geometries and stabilities

We first present the results obtained for palladium monomer and dimer and then compare them with the reported experimental and theoretical values. Our results showed that the singlet is the lowest energy state for Pd atom, and it is 0.88 eV lower in energy than that of the triplet state. This value is in close agreement with the previous theoretical values of Valerio and Toulhoat [37] and experimental value of 0.82 eV by Moore [38]. The calculated bond length, binding energy per atom, and vibrational frequency for Pd_2 are 2.58 Å, 0.50 eV, and 162.7 cm^{-1}, respectively. These GGA values are also in line with the ones carried out by Seminario et al. [39] ($R_e = 2.56$ Å, $E_b = 0.51$ eV and $\upsilon = 190$ cm^{-1}). The BLYP/DNP level of calculations by Kalita and Deka [9] gives similar values with $R_e = 2.54$ Å and $E_b = 0.55$ eV. We got similar low-lying structures but the spin multiplicity differs for few of the clusters, which might be due to the unrestricted level of calculations compared to them, which were done under restricted conditions.

In the present research work, it has been found from Table 1 that most of the isomers are stable in low-spin multiplicities. For pure and doped neutral clusters, mostly the singlet state gives the lowest energy isomers. The ionic counterparts are stable mostly in spin doublet state.

3.1.1 Neutral clusters

From Table 1, the most stable structure of PdSi is singlet with a symmetric point group of $D_{\infty h}$, same with the result of Wang and Han [40], having a bond length 2.22 Å. For Pd_2Si, the lowest energy isomer is a C_{2v} isosceles triangle in spin singlet, similar to those found by Li and co-workers [39]. The Pd–Si and Pd–Pd bond lengths in Pd_2Si are found to be 2.31 and 2.72 Å, respectively. The ground-state isomer of Pd_3Si is a C_{3v} trigonal pyramid in a singlet electronic state with the Si atom at the apex. This four-atom system is the smallest cluster that displays the appearance of a three-dimensional geometry for Pd_nSi ($n = 1$–7) clusters, which is obtained by doping a Si atom to the tetrahedral Pd_4. It is different from the analogous $TiSi_3$ for which a triplet ground state has been derived, but with similar geometric arrangement[28]. The average Pd–Si and Pd–Pd bond lengths are 2.38 and 2.76 Å, respectively. For Pd_4Si, the predicted lowest energy isomer is in spin singlet with geometry of C_{2v}. With the Si atom on an equilateral position, the average bond lengths of Pd–Si and Pd–Pd of this distorted trigonal bipyramidal isomer are 2.41 and 2.80 Å, respectively.

The most stable structure of neutral Pd_5Si is a singlet with C_{4v} symmetry, and it is a distorted octahedron obtained by placing one Si atom at the equilateral position of octahedral Pd_6. The average Pd–Si and Pd–Pd bond lengths are, respectively, 2.42 and 2.80 Å.

The ground-state structure obtained for Pd_6Si is a singlet with pentagonal bipyramid (PBP) structure. This low-lying structure has a C_{2v} symmetry with Si atom on an equatorial vertex obtained by replacing one Pd atom from PBP Pd_7. The Pd–Si and Pd–Pd bond lengths are 2.36, 2.42 Å and 2.75, 2.90 Å, respectively.

A singlet spin multiplicity with C_s point group symmetry is predicted to be the lowest energy isomer of neutral Pd_7Si. The average Pd–Si and Pd–Pd are calculated to be 2.50 and 2.81 Å, respectively.

The optimized isomers can be viewed as one Si atom replacing one Pd atom at different possible vertices of the lowest energy isomers of pure form, Pd_{n+1} ($n = 1$–7). From the present research work, it is observed, for each cluster in Fig. 1a, b, that the Si atom at the highest coordinated vertex gives the stable isomer. This is true for the

Table 1 Average bond lengths D_{avg} (Å), spin multiplicity '*Multi*', total energy E_T, HOMO-LUMO gap *Eg* and Mulliken charge q (e) of Pd (q_{Pd}) and Si (q_{Si}) in the lowest energy structures of neutral, cationic and anionic Pd_{n+1} and Pd_nSi clusters on left and right hand side of the table, respectively

Clusters	D_{avg}	Multi	E_T	E_g	Clusters	D_{avg}[a]	Multi	E_T (eV)	E_g	q_{Pd}	q_{Si}
Neutral											
Pd_2	2.58	Triplet	−278,557.43	1.99	PdSi	2.22	Singlet	−147,159.80	−1.16	−0.18	0.18
Pd_3	2.65	Singlet	−417,837.06	2.00	Pd_2Si[a]	2.31/2.72	Singlet	−286,429.53	−0.87	−0.14	0.28
Pd_4	2.72	Triplet	−557,116.80	1.95	Pd_3Si	2.38/2.76	Singlet	−425,699.23	−1.11	−0.11	0.33
Pd_5	2.75	Singlet	−696,396.50	1.09	Pd_4Si	2.37/2.78	Singlet	−564,968.86	−0.63	0.12	0.39
Pd_6	2.75	Singlet	−835,676.38	1.14	Pd_5Si	2.42/2.79	Singlet	−704,238.62	−1.77	−0.09	0.38
Pd_7	2.76	Singlet	−974,956.13	0.81	Pd_6Si	2.39/2.80	Singlet	−843,508.08	−0.50	−0.12	0.38
Pd_8	2.76	Singlet	−1,114,236.00	0.61	Pd_7Si_3	2.46/2.81	Singlet	−982,777.81	−1.50	−0.13	0.57
Cationic											
Pd_2	2.69	Doublet	−278,549.76	−0.94	PdSi	2.25	Doublet	−147,152.2242	−0.38	0.25	0.75
Pd_3	2.68	Doublet	−417,829.95	−2.47	Pd_2Si	2.32/2.76	Doublet	−286,422.3611	−0.24	0.18	0.64
Pd_4	2.72	Doublet	−557,110.17	−2.71	Pd_3Si	2.39/2.78	Doublet	−425,692.3526	−0.99	0.14	0.59
Pd_5	2.75	Doublet	−696,390.04	−1.40	Pd_4Si	2.40/2.80	Doublet	−564,962.2489	−0.11	0.11	0.55
Pd_6	2.76	Doublet	−835,670.00	−1.42	Pd_5Si_5	2.42/2.81	Doublet	−704,232.1221	−0.73	0.16	0.53
Pd_7	2.76	Doublet	−974,949.86	−1.00	Pd_6Si	2.39/2.82	Doublet	−843,501.7927	−0.46	0.14	0.53
Pd_8	2.77	Doublet	−1,114,229.80	−0.63	Pd_7Si_3	2.47/2.84	Doublet	−982,771.6725	−1.65	0.13	0.61
Anionic											
Pd_2	2.65	Doublet	−278,558.35	−1.46	PdSi	2.27	Doublet	−147,160.523	−0.45	−0.6	−0.39
Pd_3	2.7	Doublet	−417,838.19	−1.27	Pd_2Si	2.33/2.79	Doublet	−286,430.6153	−0.19	−0.46	−0.07
Pd_4	2.75	Doublet	−557,118.04	−1.41	Pd_3Si	2.39/2.80	Doublet	−425,700.5461	−0.14	−0.37	0.10
Pd_5	2.77	Doublet	−696,397.99	−0.08	Pd_4Si	2.44/2.80	Doublet	−564,970.3438	−0.11	−0.35	0.24
Pd_6	2.76	Doublet	−835,677.93	−0.77	Pd_5Si	2.42/2.82	Doublet	−704,240.1133	−1.52	−0.27	0.26
Pd_7	2.77	Doublet	−974,957.92	−0.85	Pd_6Si	2.38/2.82	Doublet	−843,509.7639	−0.73	−0.27	0.23
Pd_8	2.76	Doublet	−1,114,237.90	−1.38	Pd_7Si_3	2.49/2.83	Doublet	−982,779.5536	−1.26	−0.29	0.53

All energies are in eV

[a] The D_{avg} values for Pd_nSi clusters: Pd–Si distance/Pd–Pd distance in Å

clusters from Pd_5–Pd_8 (except Pd_7), and for the smaller clusters all the vertices are indistinguishable. Earlier it was found by Kalita and Deka [6] that the stability of the clusters increases as the coordination number increases. Here, we found that the doped atom is stable at the vertex where it has highest coordination with the neighboring atoms. This may be due to the fact that increase in the number of nearest neighbors promotes greater interactions.

3.1.2 Ionic clusters

The geometrically most stable ionic (cationic and anionic clusters obtained by removing and adding one electron from the stable neutral cluster, respectively) clusters for Pd_{n+1} and Pd_nSi ($n = 1$–7) are shown in Fig. 1. Here we have considered the cationic and anionic clusters formed by the removal and addition of an electron from the lowest energy isomers of pure and doped neutral clusters. These ionized clusters have been optimized under symmetry unrestricted conditions in three different spin multiplicities (doublet, quartet, and sextet). For both doped and pure ionic clusters, it has been found from Table 1 that the most stable structures are doublets ($M = 2$). The quintet-doublet energy separation for Pd^+ and Pd^- is 3.06 and 3.97 eV, respectively. These values are less than the earlier reported values of 3.31 and 4.78 eV, respectively, by Kalita and Deka [6].

As an overview of all optimized structures, it is obtained that the ground state of Pd_nSi^q ($n = 1$–7 and $q = 0, +1, -1$) clusters, except for Pd_6Si, the Si atom prefers the highest coordinated site. Besides, the lowest energy clusters adopt a 3D structure with low-spin multiplicity for $n = 3$–7. The ground-state geometry of the doped clusters is different from their corresponding pure clusters. In other words, doping with a single impurity atom dramatically affects the geometries of the ground-state pure neutral and ionic clusters. However, due to addition or removal of an electron from the pure as well as doped clusters, no change in geometrical structure is observed. From the discussions in Sects. 3.1.1 and 3.1.2 and taking into considerations Fig. 1a, b,

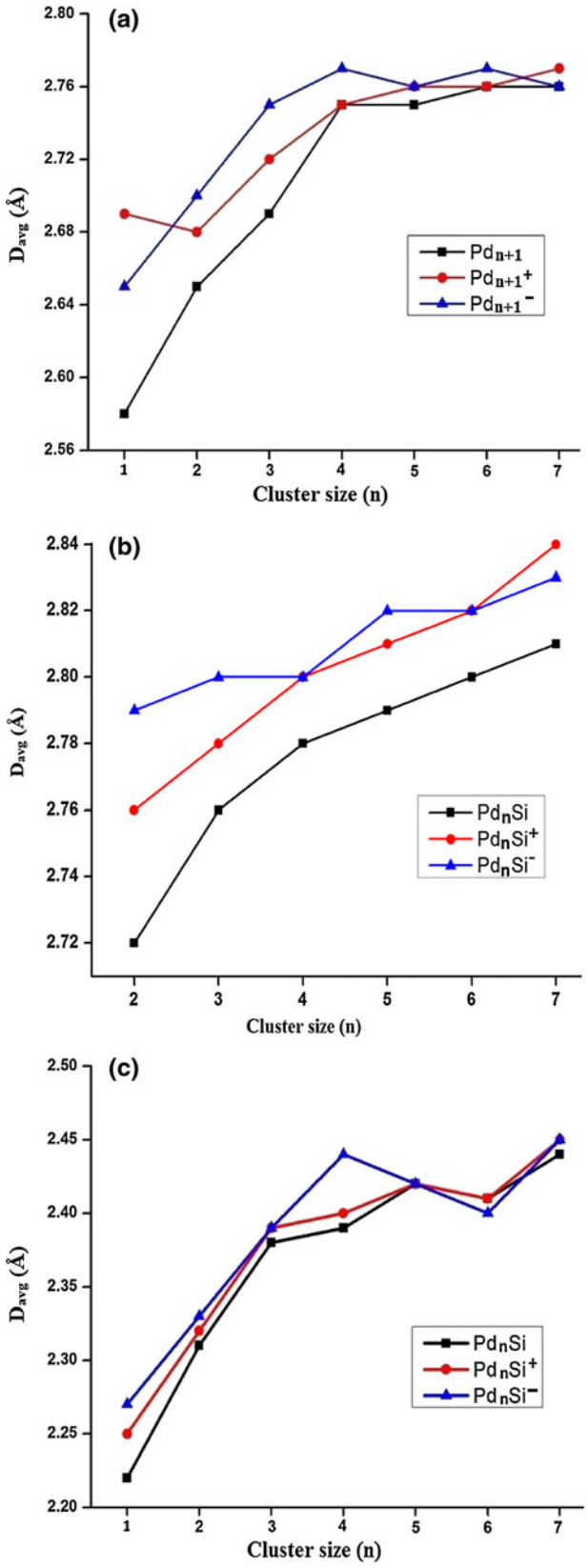

Fig. 2 Average Pd–Pd bond lengths for the most stable clusters as a function of cluster size for **a** pure and **b** doped palladium clusters, and Pd–Si bond length for **c** doped clusters

it is seen the change in charge of the cluster; as a result of addition or removal of an electron, the structure gets somewhat distorted due to change in bond length but the overall structure remains the same, i.e., no change in point group symmetry taking place, as shown in Table S2 of supporting information.

3.2 Variation of average bond length

The variation of average Pd–Pd and Pd–Si bond lengths of the lowest energy structures as a function of cluster size is shown in Fig. 2. In Fig. 2a, the average Pd–Pd bond length is found to increase as we go from Pd_2^q to Pd_5^q ($q = 0, -1$). For Pd_6^q, there is a slight decrease and then a modest increase is seen. For the cationic clusters, however, the bond length decreases for $n = 1$–2, a steady increase is seen till it reaches $n = 6$ accompanied by a small decrease for $n = 7$. The variation of average Pd–Pd bond lengths in our calculation is slightly different for the smaller clusters from that reported by Kalita and Deka [6]. They found D_{avg} decreases for $Pd_3^q(q = 0, +1, -1)$. However, the same trend is followed for all the other clusters.

In Fig. 2b, the average Pd–Pd bond length for the doped clusters shows a steady increase as we go from smaller to larger clusters. In Fig. 2c, the variation of average Pd–Si bond length is plotted as a function of cluster. The D_{avg} increases sharply from $PdSi^q$ to Pd_3Si^q ($q = 0, +1, -1$). Then, there is an even–odd alteration for the neutral and cationic clusters, due to the distortion of cluster.

The outcome displays an increment of the average bond lengths with increasing cluster size and coordination number, demonstrating the onset of three-dimensional structure. The increment becomes steady as we move to the larger clusters, as for the larger clusters the increase in coordination number will also be steady.

3.3 Relative stabilities

In order to analyze the stability and size-dependent properties of the most stable $Pd_nSi/Pd_nSi^+/Pd_nSi^-$ ($n = 1$–7) clusters, we have calculated the binding energies per atom (E_b), fragmentation energies (D) and second-order difference of energies (Δ^2E). The total energy E_T in eV for the lowest energy structures of neutral, cationic, and anionic Pd_{n+1} and Pd_nSi clusters at different spin states is given in Table S1 of supporting information, and properties of the most stable spin states are summarized in Table 1. All of the above calculations are compared with their pure counterparts concerning the influence of impurity atom on the pure nanoclusters. In cluster physics, the above stated parameters are established to be a powerful tool to reflect the relative stabilities of the clusters. In addition, the

second-order difference of energies ($\Delta^2 E$) can be compared with the relative abundances determined in mass spectroscopy experiment.

Binding energies per atom (E_b), fragmentation energies (D), and second-order difference of energies ($\Delta^2 E$) values for doped $Pd_nSi^{0,-,+}$ clusters are defined using the following formulae [34, 41]:

$$E_b(Pd_nSi^q) = [E(Si^q) + nE(Pd) - E(Pd_nSi^q)]/(n+1)$$

$$D(Pd_nSi^+) = [E(Pd_{n-1}Si^q) + E(Pd) - E(Pd_nSi^q)]$$

$$\Delta^2 E(Pd_nSi^q) = [E(Pd_{n-1}Si^q) + E(Pd_{n+1}Si) - 2E(Pd_nSi^q)]$$

For pure $Pd_n^{0,+1,-1}$ clusters, binding energies per atom (E_b), fragmentation energies (D), and second-order difference of energies ($\Delta^2 E$) are defined as the formulae followed [34, 41]:

$$E_b(Pd_{n+1}) = [(n+1)E(Pd) - E(Pd_{n+1})]/(n+1)$$

$$E_b(Pd_{n+1}^q) = [E(Pd^q) + nE(Pd) - E(Pd)]/(n+1)$$

$$D\left(Pd_{n+1}^q\right) = \left[E\left(Pd_n^q\right) + E(Pd) - E\left(Pd_{n+1}^q\right)\right]$$

$$\Delta^2 E\left(Pd_{n+1}^q\right) = \left[E\left(Pd_n^q\right) + E\left(Pd_{n+2}^q\right) - 2E\left(Pd_{n+1}^q\right)\right]$$

where $E(M)$ represents the ground-state energy of the M entity; q is the charge on the cluster, $q = 0$, $+1$ and -1 for neutral, cationic, and anionic clusters, respectively; n is the number of palladium atoms associated with the cluster.

3.3.1 Binding energies per atom

The variation of calculated binding energies per atom (E_b) for the most stable isomers as a function of cluster size is shown in Fig. 3. It is observed that the per atom binding energy for the pure cluster increases with cluster size; therefore, the clusters continue to gain energy during the growth process. However, the doped clusters show some variations and the primary conclusions can be made as follows: (1) For pure palladium clusters, Fig. 3a illustrates that the binding energy has an increasing tendency with the number of atoms in the cluster but the increment becomes slow toward the bigger sized clusters. It reflects the fact that bigger the sizes of the clusters, the more stable the molecular properties of the clusters. Comparing the three curves, it is found that the cationic clusters have highest E_b values, followed by anionic and then neutral clusters, which means that addition as well as removal of an electron enhances cluster stability. Thus, the order followed is $E_b^{cat} > E_b^{an} > E_b^{neu}$. (2) For doped clusters, the E_b value increases from $n = 1$–3 for charged clusters and then a slight odd–even effect is seen. Therefore, at $n = 3$, a visible peak occurs, signifying that the ionized $Pd_3Si^{\pm}$ cluster is more stable in the region of $n = 1$–7. But for the neutral clusters, the E_b value decreases with cluster size. It decreases steeply from $n = 1$–3 and then becomes slow for the bigger ones. However, comparing the three curves, the values get reversed from those of the pure clusters. The trend followed is $E_b^{neu} > E_b^{cat} > E_b^{an}$. (3) Nevertheless, the E_b values for $Pd_nSi^{0,\pm}$ clusters are significantly higher than those of corresponding $Pd_n^{0,\pm}$ clusters, signifying that the impurity atom improves the stability of small palladium clusters.

3.3.2 Fragmentation energies

In Fig. 4a, b, the fragmentation energies with respect to single palladium dissociation are plotted against the total number of atoms in Pd_{n+1} and Pd_nSi, respectively. The fragmentation energies are sensitive to the relative stabilities that can be observed in mass abundance spectra.

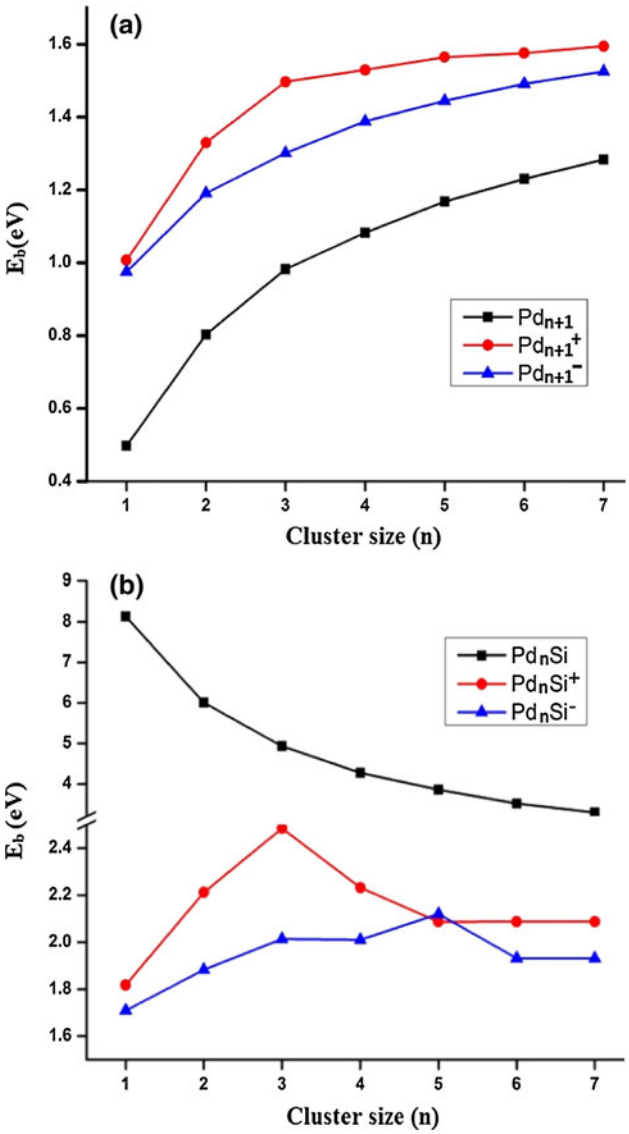

Fig. 3 Binding energies per atom E_b (eV) for the most stable clusters as a function of cluster size for **a** pure and **b** doped palladium clusters

For Pd_{n+1}^{q} ($q = 0, +1, -1$) clusters, Fig. 4a shows that cluster stabilities exhibit an odd–even oscillation as a function of cluster size. It indicates that clusters with even number of atoms are more stable than that with odd number of atoms for cationic and neutral clusters. However, the reverse is observed for the anionic clusters and the clusters bearing odd number of atoms are more stable. Among the three curves, the cationic clusters have highest values with larger peak at $n = 3$, indicating Pd_4^+ is the most stable one.

For Pd_nSi clusters, Fig. 4b shows that the fragmentation energy decreases with increasing cluster size. $Pd_2Si^{0,+,-}$ clusters have higher values, affirming that clusters at size $n = 2$ are more stable than their counterpart at $n = 3$, 4 and those at $n = 5$ and 7 are more stable at $n = 6$.

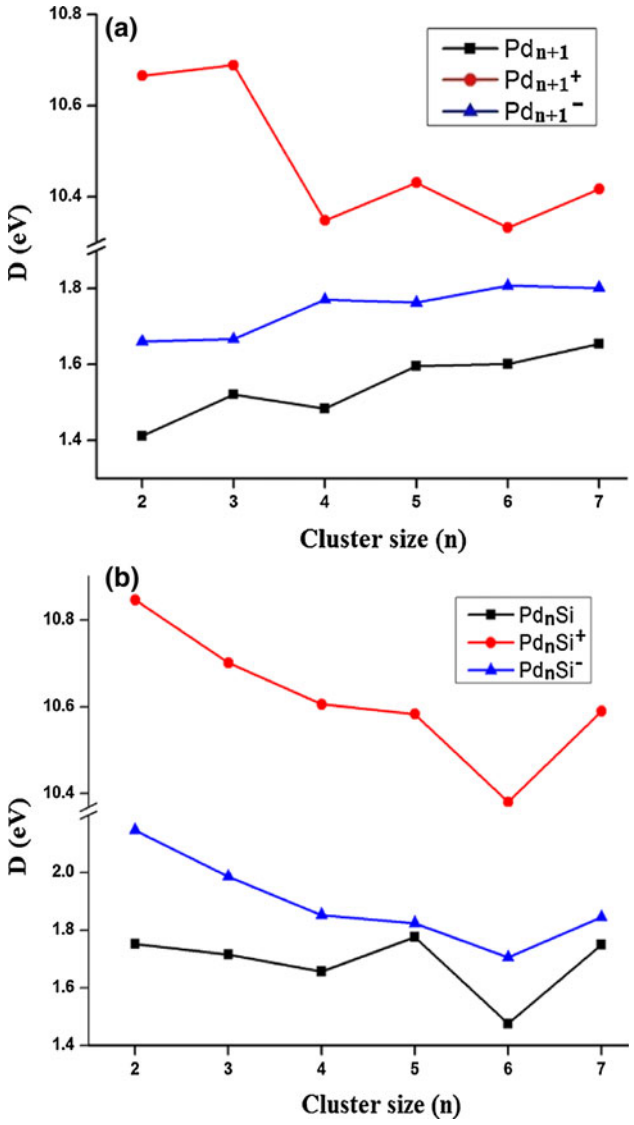

Fig. 4 Fragmentation energies per atom D (eV) as a function of cluster size for the most stable **a** pure and **b** doped palladium clusters

Meanwhile, clusters at $n = 6$ are susceptible to undergo chemical reactions. It is known that the larger the fragmentation energies are, the more difficult to set the clusters apart and thus the more stable the related clusters are. Predictably; $Pd_4^+/Pd_4/Pd_8^-$ and $Pd_2Si^{0,+,-}/Pd_5Si^{0,+,-}/Pd_7Si^{0,+,-}$ may have higher abundance in the mass spectrum.

3.3.3 *Second-order difference of energies*

The second-order difference of energies ($\Delta^2 E$), commonly known to provide the relative stability of a cluster of size n with respect to its neighbor, is provided in Fig. 5 for the most stable clusters. In Fig. 5a, the plot shows an odd–even alteration with even numbered clusters having larger $\Delta^2 E$ for the neutral as well as cationic clusters having prominent peaks at $n = 3$ and a smaller one at $n = 5$. The trend gets reversed for the anionic clusters. Among the three curves, the cationic clusters having larger values with Pd_4^+ bear the highest value, implying that Pd_4^+ is the most stable cluster.

For the doped clusters also an odd–even oscillation is seen with a maxima at $n = 5$. The same result has been observed for fragmentation energies, meaning the $Pd_5Si^{0,+,-}$ clusters, with the cationic cluster bearing the highest value, possess higher stability than their neighbors. Among the doped clusters, the neutral ones have the highest value.

3.4 Electronic properties

3.4.1 *HOMO–LUMO gaps*

The highest occupied–lowest unoccupied molecular orbital (HOMO–LUMO) energy gap is a characteristic quantity of electronic structure of clusters. It can provide an important criterion to reflect the ability of the molecule to participate in a chemical reaction, i.e., wider the HOMO–LUMO energy gap, higher the stability and abundance. On the other hand, small value is related to a high chemical activity. For low-lying configuration of Pd_{n+1} and Pd_nSi ($n = 1$–7) clusters, the difference between the eigenvalues of HOMO and LUMO is summarized in Table 1; meanwhile, Fig. 6 gives the HOMO–LUMO energy gaps of the ground-state isomers. A prominent peak is found at $n = 3$ in Fig. 6a with Pd_4^+ bearing the highest value, manifesting that they are relatively weaker in chemical activity than their neighboring clusters, whereas $Pd_5^{0,+,-}$ are active chemically and Pd_5^- being the most active one.

Pd_nSi clusters in Fig. 6b exhibit an odd–even alteration for the neutral, cationic and larger, $n \geq 4$, anionic clusters.

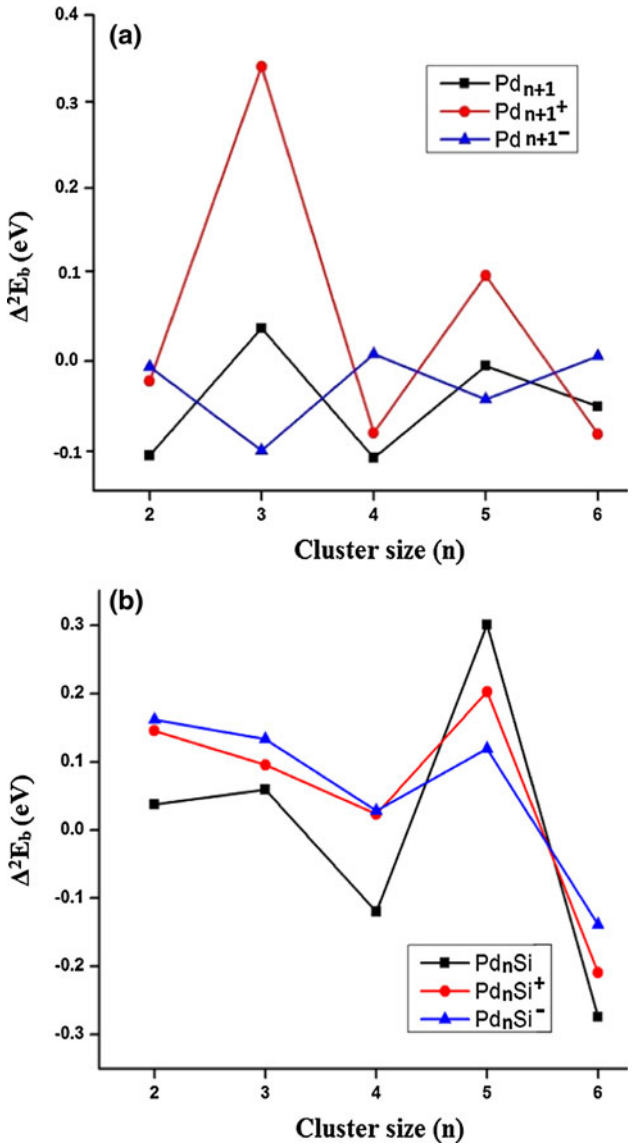

Fig. 5 Second-order difference of energies $\Delta^2 E_b$ (eV) as a function of cluster size for the most stable **a** pure and **b** doped palladium clusters

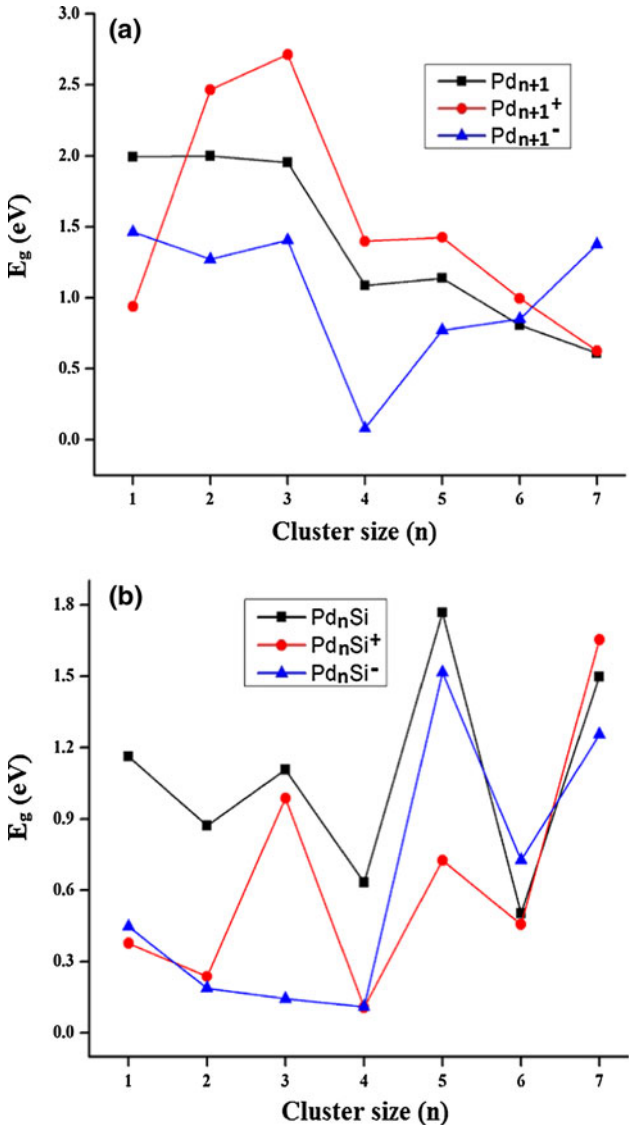

Fig. 6 HOMO–LUMO energy gaps in eV as a function of cluster size for the most stable **a** pure and **b** doped palladium clusters

Distinct cluster intensity peaks are observed at $n = 5$ and 7, indicating that these clusters are stable, whereas $Pd_4Si^{+,-}$ clusters are reactive chemically. The distribution of electron density of HOMO states of some Pd_{n+1} and Pd_nSi clusters is shown in Fig. 7. Investigating into the frontier orbitals, it is found that they consist mainly of 3*d*, 4*s*, and 4*p* states of palladium metal, which are mixed with 3*s* and 3*p* states of Si in the doped clusters. The change in HOMO–LUMO gap due to doping should be associated with the hybrid states. Owing to the significant *s*–*d* hybridization in palladium, the Fermi level consists mainly of *d*-like states in the pure clusters and combined with the *s* and *p* orbitals of silicon in the doped clusters. We hope that our results will be further confirmed by experimental studies.

3.4.2 *Charge*

The electronic properties are also discussed by probing into the Mulliken atomic charge localization. From Table 1, it is seen that for the ground-state Pd_{n+1} and Pd_nSi, the Si atoms have positive values of charges, while for Pd atom, the charge values are negative in most of the cases. However, positive charge values for palladium atoms are found for the cationic clusters but much smaller compared to that of Si atom. This suggests that there is transfer of charges in the corresponding isomer from Si atom to Pd_n

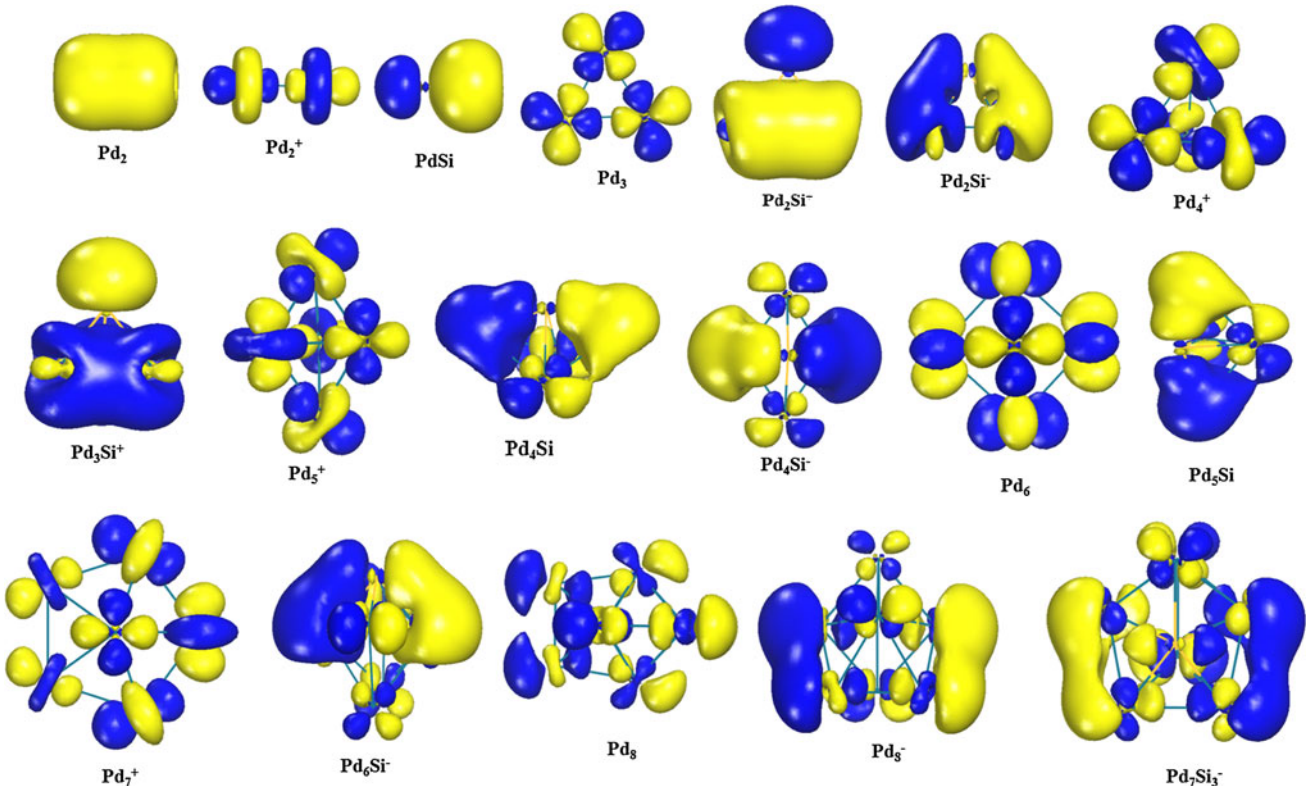

Fig. 7 The HOMO orbitals of Pd_{n+1}^{q} ($n = 1$–7 and $q = 0, +1, -1$) and Pd_nSi^q ($n = 1$–7 and $q = 0, +1, -1$) clusters

frame, which may arise due to larger electronegativity of Pd (2.20) as compared to Si (1.90), a direct consequence of relativistic effect.

4 Conclusions

We have presented an intensive study in geometrical structure, relative stabilities, and electronic properties of Pd_nSi ($n = 1$–7) clusters, and their comparison with those of their single components. Using DFT based on GGA at the BLYP/DNP level of theory, the stable isomers of neutral and charged Si-doped palladium clusters are obtained by doping Si atom in the corresponding bare Pd_{n+1} clusters under several spin state configurations. The resulting Pd_nSi have distorted geometries; however, adding or removing an electron does not change the ground-state structure with a slight distortion as a whole. The main conclusions are summarized as follows:

1. The minimum energy structures for Pd_{n+1} and Pd_nSi show the appearance of three-dimensional (3D) structure for $n = 3$–7 with the Si atom occupying the highest coordinated site.
2. The relative stabilities as a function of cluster size are studied in detail in terms of binding energy per atom, fragmentation energies, second-order difference of energies, and HOMO–LUMO gaps. The calculated results reveal that $Pd_4^+/Pd_4/Pd_8^-$ and $Pd_5Si^{0,+,-}/Pd_7Si^{0,+,-}$ have dramatically enhanced chemical stability. Besides, the clusters Pd_5^- and $Pd_4Si^{+,-}$ have small HOMO–LUMO gaps, testifying to be reactive toward chemical reactions. Moreover, the doped clusters have higher binding energy per atom, demonstrating that the bimetallic systems show enhanced chemical properties than those of their pure counterparts.
3. On the basis of electronic structure, it is evident that in the Pd_nSi configurations, Si atom acts as an electron donor, and transfer of charge between *s*, *p* and *d* states contributes to the cluster properties.

The detailed investigation into structure, stability, and electronic properties of small bimetallic clusters in the present research work will provide an insight into understanding intricate and larger doped clusters of palladium as well as other metals.

Acknowledgments This project is funded by the Department of Science and Technology, New Delhi. One of the authors P. B. is thankful to Department of Science and Technology, New Delhi, for providing INSPIRE Fellowship. The financial support in the form of Junior Research Fellowship to D. B. from Council of Scientific and Industrial Research, New Delhi, and Dr. D. S. Kothari Post doctoral fellowship to B. K. M. from University Grants Commission, New Delhi, are also acknowledged.

References

1. Kondow T, Mafune F (2003) Progress in experimental and theoretical studies of clusters. World Scientific Publishing Co. Pvt. Ltd, Singapore
2. Chen M, Kumar D, Yi C-W, Goodman DW (2005) The promotional effect of gold in catalysis by palladium–gold. Science 310:291–293
3. Maroun F, Ozanam F, Magnussen OM, Behm RJ (2001) The role of atomic ensembles in the reactivity of bimetallic electrocatalysts. Science 293:1811–1814
4. Ciuparu D, Lyubovsky MR, Altman E, Pfefferle LD, Datye A (2002) Catalytic combustion of methane over palladium-based catalyst. Catal Rev Sci Eng 44:593–649
5. Penner S, Bera P, Pedersen S, Ngo LT, Harris JJW, Campbell CT (2006) Interaction of O_2 with Pd nanoparticles on α-Al_2O_3 (0001) at low and high O_2 pressures. J Phys Chem B 110:24577–24584
6. Ong SV, Khanna SN (2011) Origin of oxidation and support-induced structural changes in Pd_4 clusters supported on TiO_2. J Phys Chem C 115:20217–20224
7. Palladium. http://en.wikipedia.org/wiki/Palladium#cite_note-37. Accessed May 2 2013
8. Tsuji J (2006) Palladium reagents and catalysts: new perspectives for the 21st century. Wiley, England
9. Kalita B, Deka RC (2007) Stability of small Pd_n (n = 1–7) clusters on the basis of structural and electronic properties: a density functional approach. J Chem Phys 127:244306–244316
10. Barman S, Kanhere DG, Das GP (2009) Enhanced magnetic moment in Fe-doped Pd*n* clusters (n = 1–13): a density functional study. J Phys Condens Matter 21:396001–396010
11. Wei L, Yao X, Tian X, Cao M, Chen W, She Y, Zhang S (2011) A DFT investigation of the effects of doped Pb atoms on Pd_n clusters ($13 \leq n \leq 116$). Comput Theor Chem 966:375–382
12. Kilimis DA, Papageorgiou DG (2010) Density functional study of small bimetallic Ag–Pd clusters. J Mol Struct THEOCHEM 939:112–117
13. Kalita B, Deka RC (2009) Reaction intermediates of CO oxidation on gas phase Pd_4 clusters: a density functional study. J Am Chem Soc 131:13252–13254
14. Ong SV, Khanna SN (2011) Theoretical studies of the stability and oxidation of Pd_n (n = 1–7) clusters on rutile TiO_2(110): adsorption on the stoichiometric surface. J Phys Chem C 116:3105–3111
15. Baber AE, Tierney HL, Sykes ECH (2010) Atomic-scale geometry and electronic structure of catalytically important Pd/Au alloys. ACS Nano 4:1637–1645
16. Peng SL, Gan LY, Tian RU, Zhao YJ (2011) Theoretical study of CO adsorption and oxidation on the gold–palladium bimetal clusters. Comput Theor Chem 977:62–68
17. Cao Y, Linde CV, Höckendorf RF, Beyer MK (2010) The $[Au_nSi]^-$, n = 1–4, potential energy surface: competition between Au–Si and Au–Au bonding. J Chem Phys 132:224307–224311
18. Majumder C (2007) Effect of Si adsorption on the atomic and electronic structure of Au_n clusters (n = 1–8) and the Au (111) surface: first-principles calculations. Phys Rev B 75:235409–235416
19. Kiran B, Li X, Zhai H-J, Cui L-F, Wang L-S (2004) [$SiAu_4$]: aurosilane. Angew Chem 116:2177–2181
20. Yang H-W, Lu W-C, Zhao L-Z, Qin W, Yang W-H, Xue X-Y (2013) Structures and electronic properties of the $SiAu_n$ (n = 17 − 20) clusters. J Phys Chem A 117:2672–2677
21. Majer K, Issendorff B (2012) Photoelectron spectroscopy of silicon doped gold and silver cluster anions. Phys Chem Chem Phys 14:9371–9376
22. Delley B (1990) An all-electron numerical method for solving the local density functional for polyatomic molecules. J Chem Phys 92:508–517
23. Delley B (2000) From Molecules to Solids with the $DMol^3$ Approach. J Chem Phys 113:7756–7764 (DMOL is a density functional theory program distributed by Accelrys Inc.)
24. Becke AD (1988) Density-functional exchange-energy approximation with correct asymptotic behavior. Phys Rev A 38:3098–3100
25. Lee C, Wang W, Parr RG (1988) Development of the Colle-Salvetti conelation energy formula into a functional of the electron density. Phys Rev B 37:785–789
26. Batista VS, Coker DF (1996) Nonadiabatic molecular dynamics simulation of photodissociation and geminate recombination of I_2 liquid xenon. J Chem Phys 105:4033–4054
27. Benedek NA, Snook IK, Latham K, Yarovsky I (2005) Application of numerical basis sets to hydrogen bonded systems: a density functional theory study. J Chem Phys 122:144102–144109
28. Inada Y, Orita H (2008) Efficiency of numerical basis sets for predicting the binding energies of hydrogen bonded complexes: evidence of small basis set superposition error compared to Gaussian basis sets. J Comput Chem 29:225–232
29. Delley B (1998) A scattering theoretic approach to scalar relativistic corrections on bonding. Int J Quantum Chem 69:423–433
30. Kalita B, Deka RC (2006) Density functional studies on structure and reactivity of Pd_n clusters for n = 1–13. Bull Catal Soc India 5:110–120
31. Cantera-López H, Montejano-Carrizales JM, Aguilera-Granja F, Morán-López JL (2010) Theoretical study of bimetallic magnetic nanostructures: Co_nPd_{N-n}, n = 0,1,…N, N = 3,5,7,13. Eur Phys J D 57:61–69
32. Li Y-F, Kuang X-Y, Mao A-J, Li Y, Zhao Y-R (2012) A DFT study on equilibrium geometries, stabilities, and electronic properties of small bimetallic Na-doped Aun (n = 1–9) clusters: comparison with pure gold clusters. J Mol Model 18:329–338
33. Wang M, Huang XW, Du ZL, Li YC (2009) Structural, electronic, and magnetic properties of a series of aluminum clusters doped with various transition metals. Chem Phys Lett 480:258–264
34. Li Y-F, Mao A-J, Li Y, Kuang X-Y (2012) Density functional study on size-selected structures, stabilities, electronic and magnetic properties of Au_nM (M = Al and Si, n = 1−9) clusters: comparison with pure gold clusters. J Mol Model 18:3061–3072
35. Deng C, Zhou L, Li G, Chen H, Li Q-S (2012) Theoretical studies on the structures and stabilities of charged, titanium-doped, small silicon clusters, $TiSi_n^-$/$TiSi_n^+$ (n = 1–8). J Clust Sci 23:975–993
36. Qin W, Lu W-C, Zhao L-Z, Zang Q-J, Wang CZ, Ho KM (2009) Stabilities and fragmentation energies of Si_n clusters (n = 2–33). J Phys Condens Matter 21:455501–455507
37. Valerio G, Toulhoat H (1996) Local, gradient-corrected, and hybrid density functional calculations on Pdn clusters for n = 1 − 6. J Phys Chem 100:10827–10830
38. Moore CE (1971) Atomic energy levels, Natl Bur Stand (U.S.). U.S. GPO, Washington, DC
39. Seminario JM, Zacarías AG, Castro M (1997) Systematic study of the lowest energy states of Pd, Pd_2, and Pd_3. Int J Quantum Chem 61:515–523
40. Wang J, Han JG (2005) Geometries, stabilities, and electronic properties of different-sized $ZrSi_n$ (n = 1–16) clusters: a density-functional investigation. J Chem Phys 123:064306–064321
41. Shao P, Kuang X-U, Zhao Y-R, Li Y-F, Wang S-J (2012) Equilibrium geometries, stabilities, and electronic properties of the cationic Au_nBe^+ (n = 1−8) clusters: comparison with pure gold clusters. J Mol Model 18:3553–3562